ABCM Symposium Series in Mechatronics - Vol. 1 - pp.428-435

MANIPULATOR CONTROL ON A MOBILE ROBOT

Marcio dos Santos Gomes
Armando Morado Ferreira
Instituto Militar de Engenharia
Departamento de Engenharia Mecânica e de Materiais
Praça General Tibúrcio, 80, CEP 22290-270
Rio de Janeiro, RJ - Brasil
marciosg@epq.ime.eb.br, armando@epq.ime.eb.br

Abstract. *We study the problem of end-effector position control of a mobile manipulator with only arm joint inputs being manipulated, as it is assumed that the wheeled platform actuation may be out of direct control. Even though such problem may be found in situations such as pointing of a robotic camera on a human-driven vehicle or platform disturbance rejection, much of the research reported in the literature assumed either fully coupled or fully decoupled control for arm and platform. We develop a fully coupled dynamic model of the mobile manipulator system, properly dealing with non-holonomic constraints, and, based on a time dependent feedback linearization scheme, we obtain a nonlinear optimal control law with arm joint inputs only. Results are illustrated by a simulated pointing control of a two degrees-of-freedom manipulator sitting on a differential drive platform.*

Keywords: *mobile manipulator dynamics, feedback linearization control.*

1. Introduction

In this work, we are interested in the control problem associated with positioning the end-effector of a mobile manipulator while its platform moves out of direct control.

The fact that a manipulator is mounted on a mobile platform greatly increases its workspace, allowing for a variety of applications such as robots for bomb squadron, search and rescue and undersea work, as well as unmanned vehicles and robotic cameras.

However, along with mobility we get some additional problems due to kinematic and dynamic coupling with the platform; namely geometric singularities, non-holonomic constraints and inertial effects.

Geometric singularities are due to redundancy between manipulator and platform motion. Dong et al (2000) studied this problem. However, this situation does not happen in our study, as the platform motion is assumed to be prescribed.

In order to deal with non-holonomic constraints in wheeled robots; some have chosen to augment the dynamic equations with the constraints (e.g., Colbaugh, 1998), while others have tried some sort of coordinate reduction after constraint augmentation (Papadopoulos et al 2000; Dong et al 2000; Yamamoto, 1996). We choose to start out with a reduced set of independent path coordinates.

Regarding to control, some of the older work was based on quasi-static assumptions for the platform (Dubowsky, 1989), and Hootsmans et al (1991) introduced suspension models into the problem. Yamamoto (1996) reported a comprehensive work, in which steps our work follows very much. Chen et al (1997) proposed an optimal trajectory generation with minimum torque and maximum manipulability as criteria. Chung et al (1999) applied robust control to a mobile manipulator with parameter uncertainties and wheel slipping. Colbaugh (1998) applied an adaptative control scheme, and Dong (2002) used the same technique for manipulator trajectory and force tracking. Papadopoulos et al (2000) reported work on simultaneous trajectory tracking for manipulator and platform, using dynamic inversion, an approach similar to the one that we present.

In this investigation we look at a particular mobile manipulator configuration: a two degrees-of-freedom manipulator, which works as a pointing device and sits on a differential-drive platform, as illustrated in Fig. (1). For this robot, we proceed a kinematics analysis to determine reference manipulator trajectories. Also, we develop a fully coupled dynamic model of the mobile manipulator system, properly dealing with non-holonomic constraints, and, based on a time dependent feedback linearization scheme, we obtain a nonlinear optimal control law with arm joint inputs only. Results are illustrated by simulations.

The paper is organized as follows. In Section 2, using the Denavit-Hartenberg convention, we develop a kinematic model of the manipulator and determine reference trajectories for the manipulator. In Section 3, we derive the manipulator dynamic model. In Section 4 we show the design of a nonlinear optimal tracking control. Section 5 shows the simulation results and comments. Finally, Section 6 presents the conclusion.

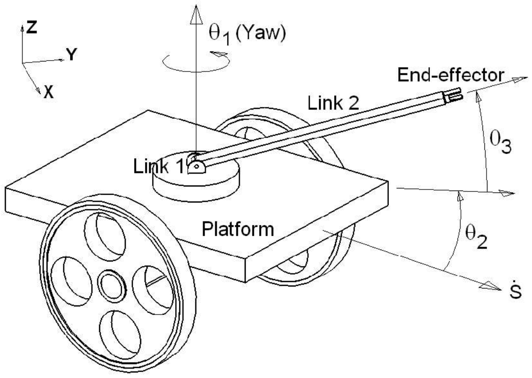

Figure 1. A 5-dof mobile manipulator.

2. Mobile Robot Kinematics

In order to determine the reference trajectories for the manipulator's joint coordinates, we look at the robot's kinematics, which we model according to the Denavit-Hartenberg convention (e.g., Spong & Vidyasagar, 1989).

In the early stage we ignore nonholonomic constraints, which are latter taken into account by properly specifying platform velocities.

Considering the robot configuration detailed in Section 1 and depicted in Fig. (1), we have the frame assignment shown in Fig. (2), to which correspond the D-H parameters of Tab. (1), where l is the arm length.

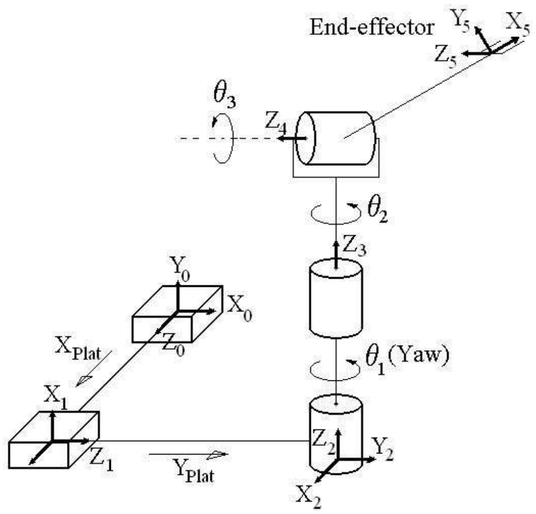

Figure 2. Mobile manipulator D-H frames.

Table 1. Mobile manipulator D-H parameters

Reference Frame	a_i	α_i	d_l	θ_i
1	0	$\pi/2$	X_{Plat}	$\pi/2$
2	0	$\pi/2$	Y_{Plat}	$\pi/2$
3	0	0	0	θ_l
4	0	$\pi/2$	0	θ_2
5	l	0	0	θ_3

Having this, we can find each homogeneous transformation from frame i to frame i-1,

$$T_{i-1}^{i} = Rot_{z,\theta_i} Trans_{z,d_i} Trans_{x,a_i} Rot_{x,\alpha_i} = \begin{bmatrix} \cos\theta_i & -\sin\theta_i \cos\alpha_i & \sin\theta_i \sin\alpha_i & a_i \cos\theta_i \\ \sin\theta_i & \cos\theta_i \cos\alpha_i & -\cos\theta_i \sin\alpha_i & a_i \sin\theta_i \\ 0 & \sin\alpha_i & \cos\alpha_i & d_i \\ 0 & 0 & 0 & 1 \end{bmatrix}, \quad (1)$$

and the full transformation from the end-effector frame to the base frame,

$$T_0^5 = T_0^1 T_1^2 T_2^3 T_3^4 T_4^5 . \tag{2}$$

Such transformation relates a target point, expressed in the end-effector frame, with its global representation:

$$\begin{bmatrix} P_{tp} \\ 1 \end{bmatrix} = T_0^5 \begin{bmatrix} \bar{P}_{tp} \\ 1 \end{bmatrix} \tag{3}$$

We are particularly interested in properly pointing the end-effector towards the target point, when we have that

$$P_{tp} = \begin{Bmatrix} x_{tp} \\ y_{tp} \\ z_{tp} \end{Bmatrix}, \bar{P}_{tp} = \begin{Bmatrix} D - C \\ 0 \\ 0 \end{Bmatrix}, \tag{4}$$

where

$$D = \sqrt{(x_{tp} - x_{Plat})^2 + (y_{tp} - y_{Plat})^2 + (z_{tp} - z_{Plat})^2} . \tag{5}$$

Therefore, by solving the inverse kinematics problem implied by Eq. (3), we can find the proper desired values for the manipulator joint coordinates to be:

$$\begin{aligned} \theta_2^{des} &= \arctan\left(\frac{(y_{tp} - y_{Plat}) \cdot \cos\theta_1 - (x_{tp} - x_{Plat}) \cdot \sin\theta_1}{(x_{tp} - x_{Plat}) \cdot \cos\theta_1 + (y_{tp} - y_{Plat}) \cdot \sin\theta_1} \right), \\ \theta_3^{des} &= \arcsin\left(\frac{z_{tp}}{D} \right). \end{aligned} \tag{6}$$

From such expressions, we can easily find its time derivatives, provided that we know the platform trajectory, which must be in accordance to its non-holonomic nature.

Having found reference trajectories for the manipulator joint coordinates, in the next section we look at its dynamics.

3. Manipulator Dynamics

We are concerned with the control of the manipulator, as we assume that the platform is out of direct control.

Nonetheless, we develop a full model of the manipulator dynamics, taking into account its coupling with the platform, in order to apply a feedback linearization scheme and derive an optimal nonlinear control law for the manipulator.

In order to deal with non-holonomic constraints in the dynamics, avoiding constraint augmentation or coordinate reduction by coordinate transformation, we choose to use path coordinates for the platform, what implicitly takes the constraints into account. Therefore, the platform coordinates are s, the length of the arc described by the robot's reference point, and θ_1, the centerline orientation angle. Hence, the velocity $\dot{s}$ is aligned with the centerline as required.

For the entire robot we have the coordinate vector given by

$$\mathbf{q} = \begin{Bmatrix} \mathbf{q}_{Plat} \\ \mathbf{q}_M \end{Bmatrix} = \begin{Bmatrix} \begin{bmatrix} s \\ \theta_1 \end{bmatrix} \\ \begin{bmatrix} \theta_2 \\ \theta_3 \end{bmatrix} \end{Bmatrix}. \tag{7}$$

With the velocities of the robot links given by

$$\mathbf{v}_{Plat} = \begin{bmatrix} \dot{s} \\ 0 \\ 0 \end{bmatrix}, \boldsymbol{\omega}_{Plat} = \begin{bmatrix} \dot{\theta}_1 \\ 0 \\ 0 \end{bmatrix}, \mathbf{v}_1 = \begin{bmatrix} \dot{s} \\ 0 \\ 0 \end{bmatrix}, \boldsymbol{\omega}_1 = \begin{bmatrix} 0 \\ \dot{\theta}_1 + \dot{\theta}_2 \\ 0 \end{bmatrix}, \tag{8}$$

$$\mathbf{v}_2 = \begin{bmatrix} \cos\theta_1\dot{s} - C\left(\sin(\theta_1+\theta_2)\cos\theta_3\dot{\theta}_1 + \sin(\theta_1+\theta_2)\cos\theta_3\dot{\theta}_2 + \cos(\theta_1+\theta_2)\sin\theta_3\dot{\theta}_3\right) \\ \sin\theta_1\dot{s} + C\left(\cos(\theta_1+\theta_2)\cos\theta_3\dot{\theta}_1 + \cos(\theta_1+\theta_2)\cos\theta_3\dot{\theta}_2 - \sin(\theta_1+\theta_2)\sin\theta_3\dot{\theta}_3\right) \\ \dot{\theta}_3\cos\theta_3 C \end{bmatrix}, \text{and}$$

$$\boldsymbol{\omega}_2 = \begin{bmatrix} \sin\theta_3\left(\dot{\theta}_1 + \dot{\theta}_2\right) \\ \cos\theta_3\left(\dot{\theta}_1 + \dot{\theta}_2\right) \\ \dot{\theta}_3 \end{bmatrix}, \tag{9}$$

we have the kinetic energy terms

$$\begin{aligned} K_{Plat} &= \frac{1}{2}M_{Plat}\dot{s}^2 + \frac{1}{2}I_{Plat}\dot{\theta}_1^2 \\ K_1 &= \frac{1}{2}M_1\dot{s}^2 + \frac{1}{2}I_1\left(\dot{\theta}_1^2 + \dot{\theta}_2^2\right) \\ K_2 &= \frac{1}{2}M_2\begin{bmatrix} \left(\cos\theta_1\cdot\dot{s} - C\left(\sin(\theta_1+\theta_2)\cos\theta_3\cdot\dot{\theta}_1 + \sin(\theta_1+\theta_2)\cos\theta_3\cdot\dot{\theta}_2 + \cos(\theta_1+\theta_2)\sin\theta_3\cdot\dot{\theta}_3\right)\right)^2 + \\ + \left(\sin\theta_1\cdot\dot{s} - C\left(-\cos(\theta_1+\theta_2)\cos\theta_3\cdot\dot{\theta}_1 - \cos(\theta_1+\theta_2)\cos\theta_3\cdot\dot{\theta}_2 + \sin(\theta_1+\theta_2)\sin\theta_3\cdot\dot{\theta}_3\right)\right)^2 + \\ \dot{\theta}_3^2\cos^2\theta_3\cdot C^2 \end{bmatrix} + \\ &+ \frac{1}{2}\left[\cos^2\theta_3\left(\dot{\theta}_1+\dot{\theta}_2\right)^2\cdot I_2 + I_2\dot{\theta}_3^2\right] \end{aligned} \tag{10}$$

where M_1, M_2, I_1 e I_2 are, respectively, masses and moments of inertia of the manipulator links 1 and 2, and C is the location of the center of mass of link 2 . Here, we also consider that link two has a symmetric cross section.

With the potential energy given by

$$\begin{aligned} V_{Plat} &= 0, \\ V_1 &= 0, \text{and} \\ V_2 &= M_2\cdot g\cdot C\cdot\sin\theta_3, \end{aligned} \tag{11}$$

where g is the gravity acceleration. Hence, we have the full robot Lagrangean and Lagrange equations

$$L_{MM} = K_{Plat} + K_1 + K_2 - V_{Plat} - V_1 - V_2 \quad . \tag{12}$$

$$\frac{d}{dt}\left(\frac{\partial L}{\partial \dot{q}_j}\right) - \frac{\partial L}{\partial q_j} = \tau_j \qquad j = 1,2,\ldots, n \ , \tag{13}$$

Considering only the manipulator dynamics, we have that the manipulator equations of motion are given by

$$\mathbf{M}_M(\mathbf{q})\ddot{\mathbf{q}}_M + \mathbf{h}_M(\mathbf{q},\dot{\mathbf{q}},\ddot{\mathbf{q}}_{Plat}) = \mathbf{u}_M \ , \tag{14}$$

where

$$\mathbf{M}_M(\mathbf{q}) = \begin{bmatrix} M_{11} & 0 \\ 0 & M_{22} \end{bmatrix}, \quad \mathbf{h}_M\left(\mathbf{q},\dot{\mathbf{q}},\ddot{\mathbf{q}}_{Plat}\right) = \begin{bmatrix} h_{11} \\ h_{21} \end{bmatrix}, \quad \mathbf{u}_M = \begin{bmatrix} \tau_2 \\ \tau_3 \end{bmatrix} \tag{15}$$

$$\begin{aligned} M_{11} &= I_1 + I_2\cos^2\theta_3 + M_2C^2\cos^2\theta_3 \\ M_{22} &= I_2 + M_2C^2 \end{aligned} \tag{16}$$

$$
\begin{aligned}
h_{11} &= \left(I_1 + I_2\cos^2\theta_3 + M_2C^2\cos^2\theta_3\right)\ddot{\theta}_1 + \\
&+ M_2C\cos\theta_3\left(\sin\theta_1\cos(\theta_1+\theta_2) - \cos\theta_1\sin(\theta_1+\theta_2)\right)\ddot{s} - \\
&- 2\sin\theta_3\cos\theta_3 I_2(\dot{\theta}_1\dot{\theta}_3 + \dot{\theta}_2\dot{\theta}_3) - M_2C\cdot\dot{s}\cdot\dot{\theta}_2\cos\theta_3(\cos\theta_1\cos(\theta_1+\theta_2) + \sin\theta_1\sin(\theta_1+\theta_2)) - \\
&- 2M_2C^2\sin\theta_3\cos\theta_3\dot{\theta}_3(\dot{\theta}_1+\dot{\theta}_2) \\
h_{21} &= \left(\sin\theta_1\sin(\theta_1+\theta_2) + \cos\theta_1\cos(\theta_1+\theta_2)\right)\left[\left(-M_2C\sin\theta_3\ddot{s}\right) - M_2\cdot\dot{s}\cdot\cos\theta_3\dot{\theta}_3C\right] - \\
&+ \cos\theta_3 I_2\sin\theta_3\left(\dot{\theta}_1^2 + \dot{\theta}_2^2\right) + 2\dot{\theta}_1\dot{\theta}_2\cos\theta_3\sin\theta_3\left(I_2 + M_2C^2\right) + \\
&+ M_2C\cdot\dot{s}\cdot\dot{\theta}_1\sin\theta_3\left(\sin\theta_1\cos(\theta_1+\theta_2) - \cos\theta_1\sin(\theta_1+\theta_2)\right) + \\
&+ M_2C^2\sin\theta_3\cos\theta_3\left(\dot{\theta}_1^2 + \dot{\theta}_2^2\right) + M_2C\cdot g\cdot\cos\theta_3
\end{aligned}
\tag{17}
$$

We notice that the manipulator dynamics shows the effects of the coupling with the platform motion. In the foregoing simulations, these equations of the manipulator's dynamics were numerically integrated by Dormand-Prince pair, an one-step method based on Runge-Kutta's 4^{th} and 5^{th} order formula.

Once the manipulator dynamics has been properly characterized, we look at the control problem in the next section.

4. Manipulator Control

In this section, based on a time dependent feedback linearization scheme, we obtain a nonlinear optimal control law for the manipulator joint inputs.

As we see, we are allowed to feedback linearize the manipulator dynamics due to its invertible structure, giving rise to a nonlinear feedback.

Having a linear representation of the dynamics, we manage to stabilize the error dynamics with gains that are optimal to a certain criteria.

As the standard techniques associated with Riccati equations showed undesirable performance for our application, an alternative method was devised for designing the linear control gains.

4.1. Feedback Linearization

In this instance, feedback linearization reduces to its particular case of dynamic inversion (Spong, Vidyasagar, 1989), also called computed torque. If we define a nonlinear feedback law

$$\mathbf{u}_M = \mathbf{M}_M(\mathbf{q})\mathbf{v} + \mathbf{h}_M(\mathbf{q}, \dot{\mathbf{q}}, \ddot{\mathbf{q}}_{Plat}), \tag{18}$$

the nonlinear dynamics of Eq. (14) becomes linear as follows:

$$\ddot{\mathbf{q}}_M = \mathbf{v}. \tag{19}$$

On choosing

$$\mathbf{v} = -K_p\mathbf{q}_M - K_v\dot{\mathbf{q}}_M + \ddot{\mathbf{q}}_M^{des} + K_v\dot{\mathbf{q}}_M^{des} + K_p\mathbf{q}_M^{des}, \tag{20}$$

where K_p and K_v are positive definite diagonal matrices, and defining the tracking error

$$\mathbf{e} = \mathbf{q}_M - \mathbf{q}_M^{des}, \tag{21}$$

the error dynamics is given by

$$\ddot{\mathbf{e}} + K_v\dot{\mathbf{e}} + K_p\mathbf{e} = 0 \tag{22}$$

Therefore, the tracking control problem now consists of finding gain matrices K_p and K_v that stabilize the error dynamics of Eq. (22).

4.2. Optimal Gains

We look for optimal gains according to quadratic criteria

$$J = \sum_{i=2}^{3} \int_{t_0}^{t_f} \left(\boldsymbol{\varepsilon}_i^T \mathbf{Q}_i \boldsymbol{\varepsilon}_i + \mathbf{w}_i^T \mathbf{R}_i \mathbf{w}_i \right) dt \, , \tag{23}$$

subject to initial conditions and

$$\begin{gathered} \dot{\boldsymbol{\varepsilon}}_i = \begin{Bmatrix} \dot{e}_i \\ \ddot{e}_i \end{Bmatrix} = \begin{bmatrix} 0 & 1 \\ 0 & 0 \end{bmatrix} \begin{Bmatrix} e_i \\ \dot{e}_i \end{Bmatrix} + \begin{Bmatrix} 0 \\ v_i - \ddot{\theta}_i^{des} \end{Bmatrix} = \begin{bmatrix} 0 & 1 \\ 0 & 0 \end{bmatrix} \cdot \boldsymbol{\varepsilon}_i + \begin{Bmatrix} 0 \\ w_i \end{Bmatrix}, \quad i = 2,3 \\ w_i = -(K_v)_i \cdot \dot{e}_i - (K_p)_i \cdot e_i \end{gathered} \tag{24}$$

The gains may be found by solving an associated Riccati equation, a well-known standard procedure in linear control (Bryson & Ho, 1969; Brogan, 1991). For a finite final time, the Riccati equation is a differential one and the optimal gains are dependent on the initial conditions and on time. In the other hand, for an infinite final time, the Riccati equation is algebraic and the gains are constant and independent both of time and initial conditions.

However, due to application demands, we would like to have very fast stabilization and low inputs at every time; and we found that this standard procedure would not give such performance. The time dependent gains are not convenient, and the constant gains resulting from the infinite final time solution are too high, causing excessively high torque for larger errors.

Therefore, an alternative procedure was sought. Taking a critically damped error dynamics as desirable, we have that

$$(K_V)_i^2 = 4(K_P)_i \tag{25}$$

With that, the analytical solution of Eq. (24) is

$$e_i(t) = e_i(0) \cdot e^{-\frac{(K_v)_i}{2} \cdot t} + \left(\dot{e}_i(0) + \frac{(K_v)_i}{2} \right) \cdot t \cdot e^{-\frac{(K_v)_i}{2} \cdot t}, \quad i = 2,3 \, . \tag{26}$$

On substituting Eq. (26) in Eq. (23), the cost, after integration, becomes a quadratic function of the gains, and the optimal values may be found by setting equal to zero the partial derivatives of the cost with respect to them:

$$\frac{\partial J}{\partial (K_v)_1} = \frac{\partial J}{\partial (K_v)_2} = 0 \tag{27}$$

5. Simulation Results

The physical properties values used in the simulation are shown in Table (2). They are similar to the ones used by Papadopoulos et al (2000), and correspond to a small size robot. Also shown are the parameters of the pointing target and maximum admissible tracking errors.

Table 2. Mobile manipulator properties and performance parameters

Mobile Manipulator		Target	
M_{Plat}(kg)	50.0	X (m)	100
I_{Plat} (kg m^2)	1.417	Y (m)	100
M_1 (kg)	3.5	Z (m)	10
I_1 (kg m^2)	0.0175	Maximum admissible errors	
M_2 (kg)	4.0	$E_{2,max}$ (rad)	0.005
I_2 (kg m^2)	0.030	$E_{3,max}$ (rad)	0.005
b (m)	0.30	Terminal time	
C (m)	0.15	t_f(s)	1.0
R_w (m)	0.10		

The chosen platform path is depicted in Fig. (4), and corresponds to a dynamically feasible trajectory of the platform assuming that the manipulator remains in its home position. Based on such trajectory, the desired state trajectories can be found as described in Section 2, so that the manipulator joint coordinates are totally prescribed.

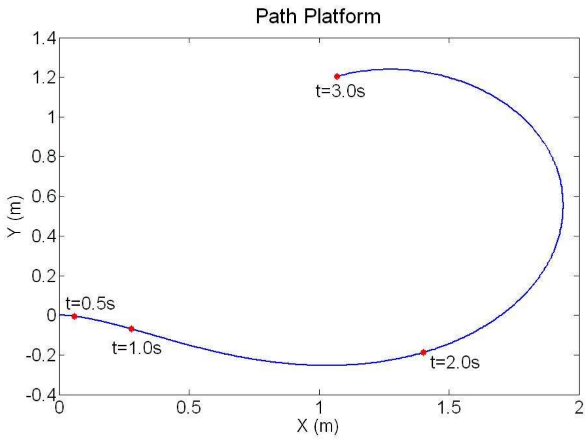

Figure 4. Mobile manipulator XY path.

As discussed in Section 4.2, we select the matrices **Q** and **R** to put more emphasis on terminal accuracy and low transient inputs, resulting on the following choice:

$$\mathbf{Q}_2 = \begin{bmatrix} 3/e^2_{2,max} & 0 \\ 0 & 1/\dot{e}^2_{2,max} \end{bmatrix}, \quad \mathbf{Q}_3 = \begin{bmatrix} 2/e^2_{3,max} & 0 \\ 0 & 1/\dot{e}^2_{3,max} \end{bmatrix} \quad \text{and} \quad \mathbf{R}_i = \begin{bmatrix} 1 & 0 \\ 0 & 1 \end{bmatrix} \tag{28}$$

Considering a worst case for the initial tracking error, when the manipulator is stationary and pointing in opposition to the target, and using the procedure described in Section 4.2, we found the optimal gains shown in Table (3). Also shown are the Riccati optimal gains for infinite final time.

Table 3. Optimal gains

	Link 1	Link 2	Link 1 (Riccati)	Link2 (Riccati)
K_p	58.93047120	39.36845645	346.4101615	282.8427125
K_v	15.35323695	12.54885755	103.4060942	102.7895200

Simulation results are shown in Fig. (5), where we show control behavior for the gains found by our procedure and the standard Riccati solution for an infinite final time. As expected, the controller attenuates the initial error, and at the specified final time (1s) both coordinate errors are within the tolerance. Also, good control action continues after 1s, despite of the platform's continuing motion.

Corresponding control torques are shown in Fig. (6). We notice a greater demand in link 1, due to its greater initial error. Also, as discussed in Section 4, the initial torques prescribed by the Riccati solution are too high, beyond acceptable limits for this application. Even though such high torques exist for a short time, failure in applying them would cause a poor control performance afterwards. Steady state values in both cases agree in following gravity and platform motion demands.

Finally, a sensitive analysis for this case showed very little variation of the optimal gains with the initial conditions.

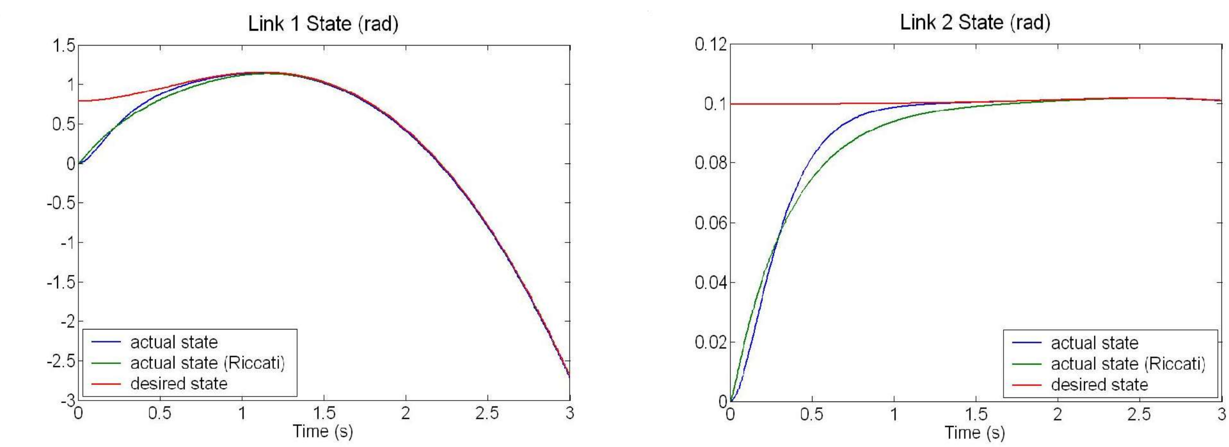

Figure 5. Comparison between desired and real states of links 1 and 2.

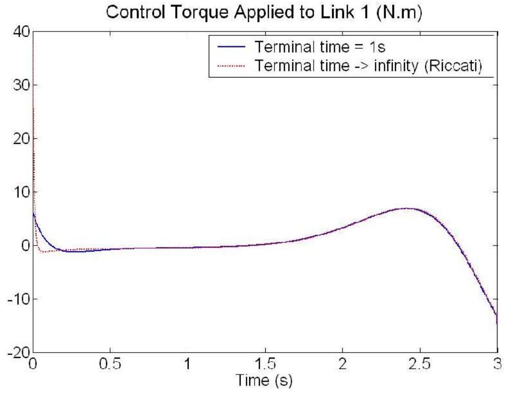

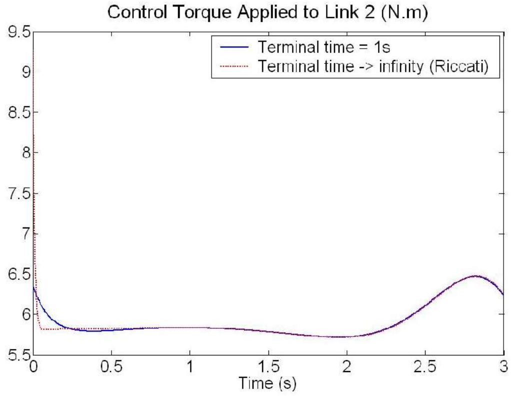

Figure 6. Input control torques for links 1 and 2.

6. Conclusion

This work focus on the problem of end-effector position control of a mobile manipulator with only arm joint inputs being manipulated, using a mobile manipulator constituted by a differential-drive platform and a two degrees-of-freedom manipulator sitting on it. A D-H kinematic formulation showed to be convenient for the problem. The proposed Lagrange formulation of the dynamics was also helpful to avoid complications coming from non-holonomic constraints, while fully accounting for it as well as for the dynamic coupling between manipulator and platform. The control problem focused on properly pointing the manipulator end-effector regardless of the platform motion, using a nonlinear optimal control based on feedback linearization. Optimal gains were found by an adaptation of standard linear control methods, resulting in good control performance according to several criteria, as evidenced out by simulated results. As a nonlinear control law, and accounting for kinematic and dynamic effects, this strategy is valid over the entire range of motions. Finally, we should point out that, despite of the relative simplicity of the robot analyzed, the approach is general and applies to other circumstances as well.

7. Acknowledgements

The authors gratefully thank the support of the Brazilian Army.

8. References

Dubowsky, S., Vance, E.E., "Planning Mobile Manipulator Motions Considering Vehicle Dynamic Stability Constraints", Proceedings of IEEE International Conference on Robotics and Automation, Scottsdale, AZ, May 14-19, 1989, pp. 1271 – 1276.

Hootsmans, N.A.M., Dubowsky, S., "Control of Mobile Manipulators including Vehicle Dynnamic Characteristics", Proceedings of the Fourth Topical Meeting on Robotics and Remote Systems, Albuquerque, NM, February 1991, pp. 461 – 470.

Hootsmans, N.A.M., Dubowsky, S., "Large Motion Control of Mobile Manipulators Including Vehicle Suspension Characteristics", Proceedings of the 1991 IEEE International Conference on Robotics and Automation, Sacramento, CA, vol. 3, April, 1991, pp. 2336 – 2341.

Yamamoto, Y., Yun, X., "Effect of the Dynamic Interaction on Coordinated Control of Mobile Manipulators", IEEE Transactions on Robotics and Automation, Vol. 12, No. 5, October 1996, pp. 816 – 824.

Colbaugh, R., "Adaptive Stabilization of Mobile Manipulators", Proceedings of the American Control Conference, Philadelphia, Pennsylvania, June, 1998, pp. 1 – 5.

Chen, M.W., Zalzala, A.M.S., "Dynamic Modelling and Genetic-Based Trajectory Generation for Non-Holonomic Mobile Manipulators", Control Engineering Practice, Vol. 5, No. 1, 1997, pp. 39 – 48.

Chung, J.H., Velinsky, S.A., "Robust Control of a Mobile Manipulator – Dynamic Modelling Approach", Proceedings of American Control Conference, San Diego, California, June, 1999, pp. 2435 – 2439.

Dong, W., Xu, Y., Wang, Q., "On Tracking Control of Mobile Manipulators", Proceedings of the 2000 IEEE International Conference on Robotics and Automation, San Francisco, CA, April, 2000, pp. 3455 – 3460.

Papadopoulos, E., Poulakakis, J., "Planning and Model-Based Control for Mobile Manipulators", Proceedings IROS 2000 Conference on Intelligent Robots and Systems, Takamatsu, Japan, 2000, pp. 1 - 6.

Dong, W., "On Trajectory and Force Tracking Control of Constrained Mobile Manipulators with Parameter Uncertainty", Automatica, No 38, 2002, pp. 1475 – 1484.

Spong, M.W., Viddyasagar, M. "Robot Dynamics and Control", John Wiley & Sons, 1989, 336 p. il., ISBN 0-471-61243-X.

Bryson, A.E., Ho, Y., "Applied Optimal Control", 1st Edition, Ginn and Company, 1969, 481 p. il.

Brogan, W.L., "Modern Control Theory", 3rd Edition, Prentice Hall, 1991, 653 p. il., ISBN 0-13-589763-7.